Spin-$\frac{1}{2}$ J_1-J_2 Heisenberg antiferromagnet on a square lattice: A plaquette renormalized tensor network study

Ji-Feng Yu
Center for Quantum Science and Engineering, National Taiwan University, No. 1, Sec. 4, Roosevelt Rd., Taipei 106, Taiwan

Ying-Jer Kao*
Department of Physics, and Center for Advanced Study in Theoretical Science, National Taiwan University, No. 1, Sec. 4, Roosevelt Rd., Taipei 106, Taiwan

(Received 22 August 2011; revised manuscript received 17 November 2011; published 5 March 2012)

We apply the plaquette renormalization scheme of tensor network states [Phys. Rev. E **83**, 056703 (2011)] to study the spin-1/2 frustrated Heisenberg J_1-J_2 model on an $L \times L$ square lattice with $L = 8$, 16, and 32. By treating tensor elements as variational parameters, we obtain the ground states for different J_2/J_1 values, and investigate staggered magnetizations, nearest-neighbor spin-spin correlations, and plaquette order parameters. In addition to the well-known Néel order and collinear order at low and high J_2/J_1, we observe a plaquettelike order at $J_2/J_1 \approx 0.5$. A continuous transition between the Néel order and the plaquettelike order near $J_2^{c_1} \approx 0.40J_1$ is observed. The collinear order emerges at $J_2^{c_2} \approx 0.62J_1$ through a first-order phase transition.

DOI: 10.1103/PhysRevB.85.094407 PACS number(s): 75.10.Jm, 75.40.Mg, 03.67.−a

I. INTRODUCTION

The search for exotic states in quantum magnets has been the topic of intensive research for the past decades. An extremely important question is when the conventional Néel order is destroyed, what kind of states can emerge. Frustrated antiferromagnetic spin systems, where the frustration from either the lattice geometry, or the presence of competing interactions, are candidate systems to study these states. It is proposed that when the Néel order is destroyed by quantum fluctuations, only short-range correlations will survive, and the system enters a quantum paramagnetic state which can be described as a resonant valence bond (RVB) state.[1] The RVB state can either be a valence bond solid (VBS) phase, where some of the lattice symmetries are broken,[2] or a featureless spin liquid with strong short-range correlations without any broken spin symmetry.[3,4] One archetypical model to study the effect of frustration from competing interactions is the antiferromagnetic (AF) J_1-J_2 Heisenberg model on a square lattice.[3,5–15] The Hamiltonian is given by,

$$H = J_1 \sum_{\langle ij \rangle} \mathbf{S}_i \cdot \mathbf{S}_j + J_2 \sum_{\langle\langle ij \rangle\rangle} \mathbf{S}_i \cdot \mathbf{S}_j, \tag{1}$$

where $J_1 > 0$ and $J_2 > 0$ are the nearest-neighbor (NN) and next-nearest-neighbor (NNN) couplings, and the sums $\langle ij \rangle$ and $\langle\langle ij \rangle\rangle$ run over NN and NNN pairs, respectively. Recent interests of this model have been revived by the discovery of Fe-based superconducting materials[16] where a weakened AF order can be described by this model with $S > 1/2$.[17–19]

Properties of this model for $S = 1/2$ in two dimensions have been studied extensively by a variety of methods, such as spin wave theory,[5] exact diagonalization (ED),[6,7,14] series expansion,[12,20–23] large-N expansion,[2] functional renormalization group,[15] Green's function method,[11] projected entangled pair states,[24] etc. It is generally believed that in the region $J_2/J_1 \lesssim 0.4$, the ground state (GS) of the model is the Néel phase with magnetic long-range order (LRO). In the region $J_2/J_1 \gtrsim 0.65$, spins in the GS are ordered at wave vector $(\pi,0)$ or $(0,\pi)$, showing so-called collinear magnetic LRO. The GS in the intermediate region is proposed to be a quantum paramagnet without magnetic LRO, but the properties of this phase are still under intensive debate. There are several proposals for the GS, such as a columnar dimer state,[21,24] a plaquette VBS order,[8,13,25] or a spin liquid.[3,4] In the meantime, precise determination of the phase transition points is also not conclusive. Earlier series expansion studies[21] estimate the quantum paramagnetic region is between $0.38 \lesssim J_2/J_1 \lesssim 0.62$. A recent ED study[14] using results of up to $N = 40$ to perform finite-size extrapolation estimates the transition points at $J_2^{c_1} \simeq 0.35J_1$ and $J_2^{c_2} \simeq 0.66J_1$. Meanwhile, studies by a combination of random phase approximation and functional renormalization group find this nonmagnetic phase begins near $J_2/J_1 \approx 0.4 \sim 0.45$ and ends around $0.66 \sim 0.68$.[15]

Numerical studies of frustrated quantum spin systems present great challenges in dimensions greater than one. The ED method is hampered by the limitation of system size one can simulate. At present, the largest system size on the square lattice that can be simulated is $N = 40$.[14,26] Due to the minus sign problem,[27] the powerful quantum Monte Carlo (QMC) method is not applicable to highly frustrated systems. In one dimension, the density matrix renormalization group (DMRG)[28] algorithm, which generates matrix product states (MPS), can reach very high accuracy even for frustrated spin systems; however, direct extension of the algorithm to higher dimensions remains difficult. One promising proposal is to generalize the MPS to higher dimensions, the tensor network states (TNS),[29–31] which can serve as potential candidates for studying these systems. In the TNSs, the matrices are replaced by tensors of rank corresponding to the coordination number of the lattice. On a two-dimensional (2D) square lattice, the tensor $T^s_{ijkl}(\sigma_s)$ on site s has four indices, in addition to the physical index, which in the current case corresponds to the z-component σ_s of a spin. Although there are both NN and NNN interactions in the Hamiltonian [Eq. (1)], we should mention that the rank of tensors in a TNS is chosen according to the coordination number of each physical lattice site.[29] In

this way, the area law of entanglement entropy is satisfied by construction. If the bond dimension D is large enough, the many-body wave function represented by a TNS should capture the entanglement in the ground state and thus gives a good approximation of the ground state.

Contracting over all bond indices gives the wave function coefficient for a given spin state $\sigma_1, \ldots, \sigma_N$.[32–34] In these tensor network-based methods, one of the major obstacles is the computational complexity involved in the tensor contraction, then usually some type of approximation is required to make the computation manageable. Several schemes have been proposed to facilitate the contraction of the tensor networks.[32–36] In particular, a contraction scheme based on the plaquette renormalization with auxiliary tensors is proposed to retain the variational nature of the method, and it is shown that for the transverse Ising model, even with the smallest possible bond dimension ($D = 2$), non-mean-field results can be obtained.[34]

In this paper, we use the TNS with the plaquette renormalization scheme to study the J_1-J_2 Heisenberg model on a square lattice. We find that even with a small bond dimension $D = 2$, it already provides a useful way to study the nature of the transition and estimate the value of the transition points. The rest of this paper is organized as follows. In the following section, we review the plaquette renormalization scheme of TNS, and how to apply the scheme to the current model. Main results will be presented in Sec. III, as well as some discussions. Sec. IV will give a brief summary.

II. METHOD

We investigate the ground state of frustrated Heisenberg J_1-J_2 model on a square lattice, using the plaquette renormalized tensor network.[34] The trial wave function is written as

$$|\Psi\rangle = \sum_{\{\sigma\}} t\mathrm{Tr}\left(T_1^{\sigma_1} \otimes T_2^{\sigma_2} \cdots\right)|\sigma_1\sigma_2\cdots\rangle, \tag{2}$$

where tTr indicates the tensor trace that all the tensor indices are summed over. T_s is rank-4 tensor on site s, with bond dimension D for each rank and $\sigma_s = \uparrow$ or $\downarrow$ is the physical spin state.

Explicit contraction of the tensor network is computationally intensive. To keep the computational complexity from growing exponentially, auxiliary rank-3 tensors A^n_{ijk} are added to each level of the contraction process (Fig. 1); each transforms and truncates a pair of indices. A sequence of plaquette renormalizations, $n = 1,2,\ldots$, is carried out and the bond dimension of each rank is thus kept constant after every plaquette contraction.[34] In order to compute physical expectation values based on a TNS, one has to contract the tensors of a bra and ket state over their physical (e.g., spin) indices in addition to the bond indices of the tensors. Normally, one would first construct the double tensors by performing the sum over the physical indices,

$$\mathbb{T}^s_{abcd} = \sum_{\sigma_s,\sigma'_s=\uparrow,\downarrow} T^{s*}_{i_2j_2k_2l_2}(\sigma'_s)T^s_{i_1j_1k_1l_1}(\sigma_s), \tag{3}$$

where the labels a,b,c,d is a suitable combination of the indices of the bra (T^{s*}) and ket (T^s) tensors [i.e., $a = i_1 + D(i_2 - 1)$, etc.] In the calculation of the matrix element

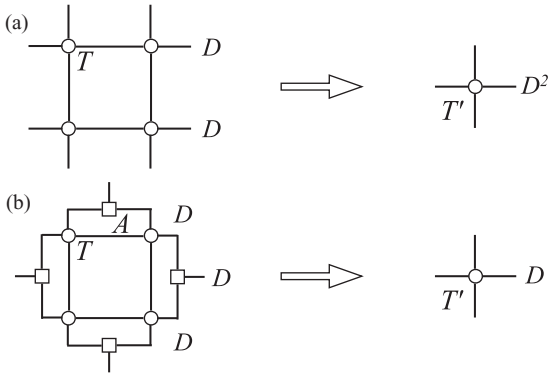

FIG. 1. (a) Direct contraction of four connecting rank-4 tensors T with bond dimensions D results in a new tensor T' with bond dimensions D^2. (b) Plaquette renormalized tensor contraction via additional auxiliary rank-3 tensors A with bond dimensions D. The resulting tensor T' has the same bond dimension D as the original tensor T.

$\langle\Psi|\hat{O}|\Psi\rangle$ of some operator involving one or several sites, similar tensors are constructed for the sites at which operators act weighted with a local expectation value $\langle\sigma'_s|\hat{O}_s|\sigma_s\rangle$. In addition, the renormalization double tensors can be also formed,

$$\mathbb{A}^n_{abc} = A^{n*}_{i_2j_2k_2}A^n_{i_1j_1k_1}. \tag{4}$$

The bond dimension of each rank in the resulting double tensor becomes $\mathbb{D} = D^2$. This renormalization scheme reduces the maximum computational complexity[34] to $\mathbb{D}^8 = D^{16}$ for a double tensor network.

The ground-state wave function can be obtained by optimizing the elements of tensors $\mathbb{T}$,$\mathbb{A}$ for the ground–state energy. Since the plaquette renormalization is introduced at the wave-function level, instead of the constructed double tensor network, the method remains variational and the final energy will give an upper bound for the true ground-state energy. We optimize the wave function using the derivative-free Brent's method.[37] Compared to previous methods involving singular value decomposition (SVD),[32,33] the environment of a given tensor is fully taken into account in the current scheme. However, the introduction of the renormalization A tensors at the wave-function level effectively reduces the maximum support of the entanglement entropy area law in this tensor network. To reduce the number of free parameters, we impose symmetries on the trial wave function. We use a single plaquette (i.e., $2 \times 2 = 4$ sites as a unit cell) (Fig. 1), wherein tensors T on each site and auxilliary tensors A_0 are assumed to be different. This unit is translated to generate a 4×4 unit and another set of auxilliary tensors A_1 are added. This procedure is repeated until the full lattice is generated. Finally, the periodic boundary condition is applied.[34]

III. RESULTS AND DISCUSSIONS

We obtain the ground-state wave function by varying the elements in the tensors T and A with $D = 2$, which describes a slightly entangled state beyond the product (mean-field) state ($D = 1$). Figure 2(a) shows the ground-state energy with system sizes $L = 8,16$, and 32. A clear cusp near

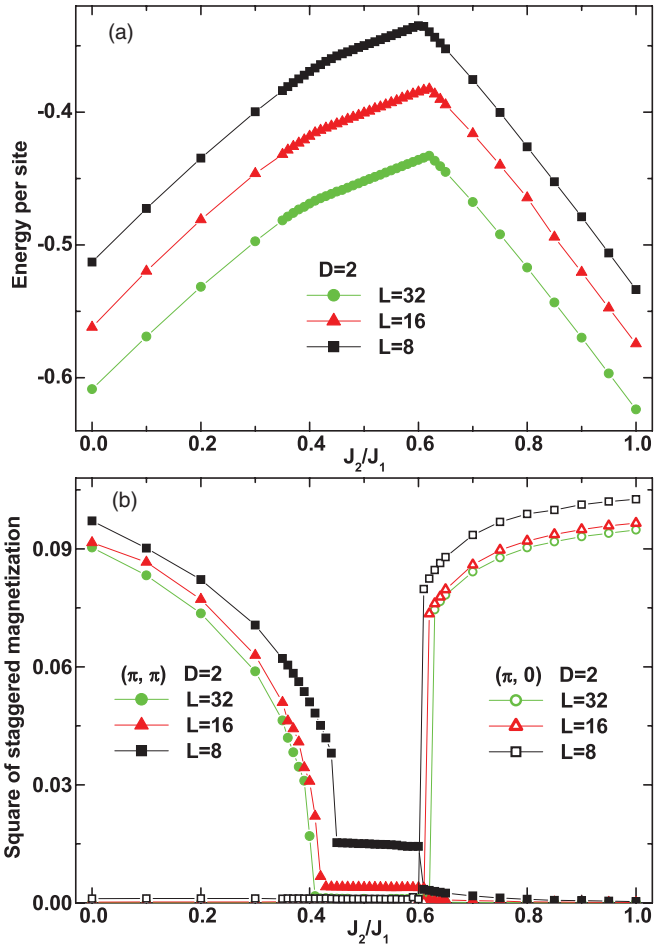

FIG. 2. (Color online) (a) The ground-state energy per site as a function of J_2/J_1. The curves for $L = 8$ and 16 are shifted up by 0.05 and 0.10 for clarity. (b) The square of staggered magnetization as a function of J_2/J_1.

$J_2/J_1 = 0.62$ is observed, signaling a first-order phase transition. A continuous change of the slope is found near $J_2/J_1 = 0.4$, probably indicating a continuous phase transition there.

To study the details of the magnetic orders and the transition points, we compute the magnetic structure factor, or the square of staggered magnetization at wave vector $\mathbf{q}$, defined as

$$M^2(\mathbf{q}) = \frac{1}{N^2}\sum_{ij} e^{i\mathbf{q}\cdot(\mathbf{r}_i-\mathbf{r}_j)}\langle \mathbf{S}_i \cdot \mathbf{S}_j\rangle, \tag{5}$$

where $\mathbf{r}_i = (x_i, y_i)$, and $\mathbf{q} = (\pi,\pi)$ for the Néel order, and $(0,\pi)$ or $(\pi,0)$ for the collinear order. $M^2(\mathbf{q})$ tends to the square of the order parameter in the thermodynamic limit if there is magnetic ordering at wave vector $\mathbf{q}$, and scales like $1/N$ in a magnetically disordered phase.

Figure 2(b) shows the results of the square of staggered magnetizations $M^2(\pi,\pi)$ and $M^2(\pi,0)$. From the small J_2/J_1 side, the Néel order is smoothly suppressed as J_2 increases, until $J_2/J_1 \simeq 0.40$, where a discontinuous jump of the Néel order is observed for $L = 8$, and the jumps become less pronounced as the system size increases. This strong size dependence of the jump is another example that in a finite-size tensor network state with finite bond dimensions, there exists two energy minima near the transition, rendering the transition first-order at small N. For a putative continuous transition, these two minima move closer to each other with increasing N and the transition becomes continuous at $N \to \infty$.[38]

From the large J_2/J_1 side, the collinear order also decreases smoothly, until $J_2/J_1 \simeq 0.6$ where a clear first-order transition occurs. Unlike the previous case, the jumps in $M^2(\pi,0)$ remain robust upon increasing N, strongly suggesting against a continuous transition here. This transition to the collinear order is consistent with previous numerical calculations.[12,14,20–23]

We now use our data from different sizes to extract the order parameters in the thermodynamic limit. This allows us to estimate the transition points between the Néel/collinear state and the nonmagnetic (disordered) phase. The finite-size extrapolation rules for the two-dimensional antiferromagnetic Heisenberg model are well known.[39–41] Following Refs. 14 and 41, we define the Néel-order parameter as $m_0 = 2\lim_{N\to\infty} M(\pi,\pi)$. This normalization is chosen so that $m_0 = 1$ in a perfect Néel state. The finite-size behavior of $M^2(\pi,\pi)$ is given by[14,41]

$$M^2(\pi,\pi) = \frac{m_0^2}{4}\left(1 + \frac{0.62075\, c}{\rho L} + \cdots\right), \tag{6}$$

where c is the spin-wave velocity and ρ is the spin stiffness. The order parameter for the collinear order is defined as $m_1 = \sqrt{8}\lim_{N\to\infty} M(\pi,0)$. The finite-size behavior of $M(\pi,0)$ is given by[14,41]

$$M^2(\pi,0) = \frac{1}{8}m_1^2 + \frac{\text{const.}}{L} + \cdots \tag{7}$$

The extra 1/2 factor comes from the fact that the ground state has an extra twofold degeneracy $\mathbf{q} = (\pi,0),(0,\pi)$, and this symmetry is broken in the thermodynamic limit. Figure 3(a) shows the extrapolated results for m_0 and m_1 as a function of J_2/J_1. We find that the GS near $J_2/J_1 = 0.5$ is magnetically disordered (i.e., both m_0 and m_1 vanish). Figure 3(b) shows the finite-size scaling of $M^2(\pi,\pi)$ and $M^2(\pi,0)$ at $J_2/J_1 = 0.5$, which both shows a $1/N$ scaling with the zero intercept as $N \to \infty$. The transition points are estimated to be $J_2^{c_1} = 0.40J_1$ and $J_2^{c_2} = 0.62J_1$, consistent with estimates from series expansion[12,20–23,42] where $J_2^{c_1} \approx 0.38J_1$ and $J_2^{c_2} \approx 0.62J_1$, and slightly different from ED results $J_2^{c_1} \approx 0.35J_1$ and $J_2^{c_2} \approx 0.66J_1$.[14] Near $J_2^{c_1}$, we fit the Néel-order parameter m_0 to a power law $m_0 \sim (J_2 - J_2^{c_1})^\beta$, and an asymptotic mean-field behavior consistent with $\beta = 1/2$ is also observed.[38] For $J_2 = 0$, we obtain $m_0 = 0.592$ which is slightly lower than the best estimate from the quantum Monte Carlo ($m_0 = 0.6140$).[43] Although it is also possible to extract c and ρ from our data based on Eq. (6), it is argued that determination of these quantities by fitting the prefactors of the leading finite-size corrections ($O(1/L)$) cannot reach the same accuracy as the magnetic order parameters.[14]

Analogous to how mean-field theory produces symmetry-broken states, this method can produce solutions which break spin-rotation symmetry on a finite lattice.[34,38] We examine the spin-rotation symmetry of the ground state, with the focus in the nonmagnetic phase. Figure 4 shows z and xy components

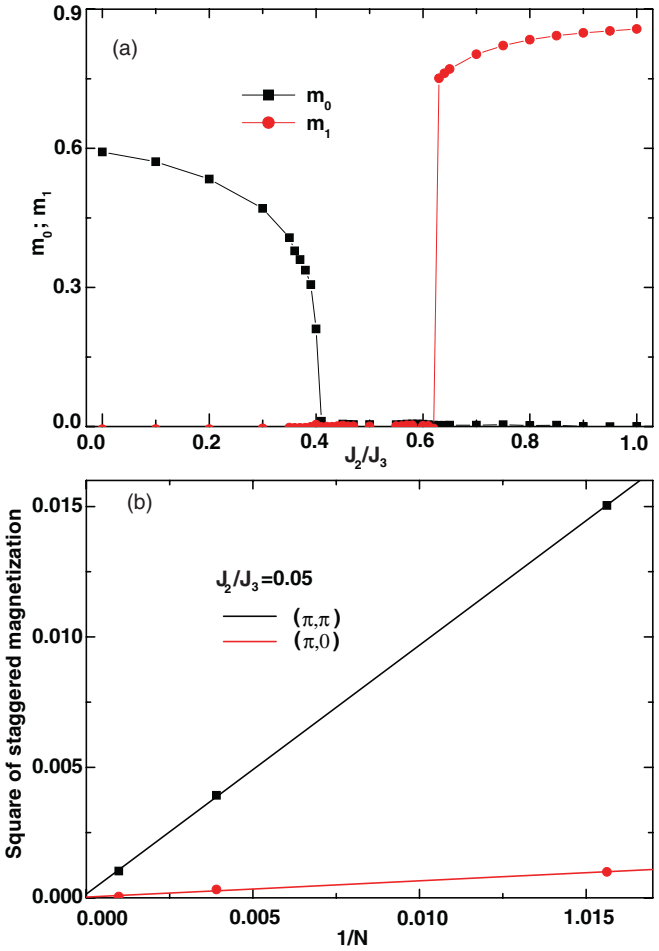

FIG. 3. (Color online) (a) Extrapolated order parameters m_0 and m_1 as a function of J_2/J_1. (b) Finite-size scaling of $M^2(\pi,\pi)$ and $M^2(\pi,0)$ at $J_2/J_1 = 0.5$, where both order parameters m_0 and m_1 scale to zero in the thermodynamic limit.

of the square of staggered magnetization at $\mathbf{q} = (\pi,\pi)$ for $L = 32$, defined as

$$M_z^2(\pi,\pi) = \frac{1}{N^2}\sum_{ij} e^{i\pi[(x_i-x_j)+(y_i-y_j)]}\langle S_i^z S_j^z\rangle,$$

$$M_{xy}^2(\pi,\pi) = \frac{1}{N^2}\sum_{ij} e^{i\pi[(x_i-x_j)+(y_i-y_j)]}\langle S_i^x S_j^x + S_i^y S_j^y\rangle.$$

For reference, the sum of the two is also included. In the Néel phase, spin-rotation symmetry is clearly broken.[34] Increasing J_2 through a phase transition to the strongly frustrated regime (i.e., $0.45 \lesssim J_2/J_1 \lesssim 0.60$), the spin-rotation symmetry is restored with $M_z^2 = \frac{1}{2}M_{xy}^2 = \frac{1}{3}M^2$, as expected.

In order to clarify the possible new phase in the highly frustrated region around $J_2/J_1 = 0.5$, we calculate the nearest-neighbor spin-spin correlations for $L = 32$. Figure 5 shows the results for $J_2/J_1 = 0.10$, which is deep inside the Néel phase, and $J_2/J_1 = 0.50$, which is in the magnetically disordered phase. The numbers in black near the bond are the NN spin-spin correlation, and the thickness of the bond is proportional to its magnitude. For $J_2/J_1 = 0.50$ [Fig. 5(b)], the NN spin-spin correlations within a single plaquette are much stronger than those between plaquettes. On the other hand, deep inside

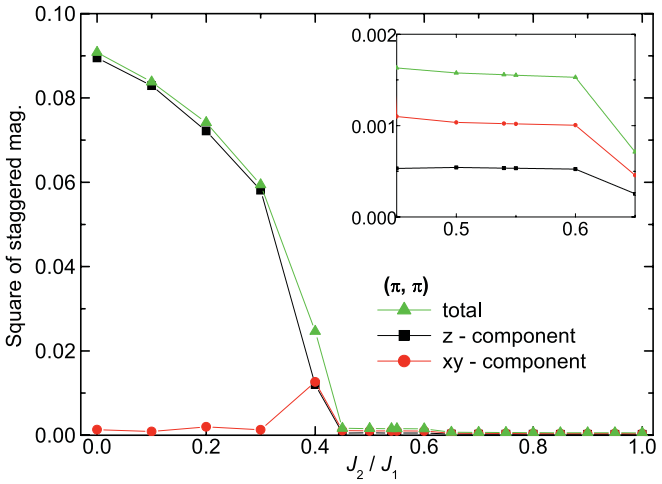

FIG. 4. (Color online) The z(black), xy(red) components of the square of staggered magnetization and the sum of the two (green) as a function of J_2/J_1. (Inset) Same quantities in the region of $J_2/J_1 = 0.45 \sim 0.65$.

the Néel phase $J_2/J_1 = 0.10$ [Fig. 5(a)], the NN spin-spin correlations show a more uniform pattern, although weaker correlations are present in some bonds between plaquettes. Overall, it is clear that the correlations inside a 2×2 plaquette become stronger upon increasing J_2/J_1, which indicates a possible plaquette order in the magnetically disordered phase.

We also investigate the plaquette order parameter, which distinguishes clearly a Néel-ordered phase from a plaquette order, defined as[24]

$$\begin{aligned} Q_{\alpha\beta\gamma\delta} &= \tfrac{1}{2}\left(P_{\alpha\beta\gamma\delta} + P_{\alpha\beta\gamma\delta}^{-1}\right) \\ &= 2[(\mathbf{S}_\alpha\cdot\mathbf{S}_\beta)(\mathbf{S}_\gamma\cdot\mathbf{S}_\delta) + (\mathbf{S}_\alpha\cdot\mathbf{S}_\delta)(\mathbf{S}_\beta\cdot\mathbf{S}_\gamma) \\ &\quad - (\mathbf{S}_\alpha\cdot\mathbf{S}_\gamma)(\mathbf{S}_\beta\cdot\mathbf{S}_\delta)] + \tfrac{1}{2}(\mathbf{S}_\alpha\cdot\mathbf{S}_\beta + \mathbf{S}_\gamma\cdot\mathbf{S}_\delta + \mathbf{S}_\alpha\cdot\mathbf{S}_\delta \\ &\quad + \mathbf{S}_\beta\cdot\mathbf{S}_\gamma) + \tfrac{1}{2}\left(\mathbf{S}_\alpha\cdot\mathbf{S}_\gamma + \mathbf{S}_\beta\cdot\mathbf{S}_\delta + \tfrac{1}{4}\right). \end{aligned} \quad (8)$$

The results of the plaquette order parameter are shown also in Fig. 5 (numbers in red italic) for $J_2/J_1 = 0.10$ and 0.50. In the most frustrated region, we observe signature of the plaquette order. For $J_2/J_1 = 0.50$, the plaquette-order parameter is much stronger within a plaquette, consistent with observation

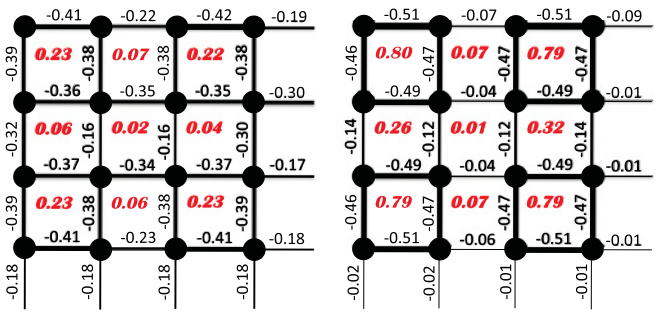

FIG. 5. (Color online) The NN spin-spin correlations $\langle \mathbf{S}_i\cdot\mathbf{S}_j\rangle$ (black numbers near bond) and the plaquette order parameter (red numbers in italic) for $J_2/J_1 =$ (a) 0.10 and (b) 0.50, with system size $L = 32$. We show only one corner (4×4) of the entire lattice as the pattern is repeated periodically.

from the spin-spin correlations. This order parameter is small in the Néel phase ($J_2/J_1 = 0.10$), although some traces of the plaquette order are still present. This might be due to the inherent structure of the renormalization scheme, which explicitly breaks the translational invariance, or possibly the plaquette correlations already start to build up in this regime. It remains to further explore whether this plaquette order is favored due to our renormalization scheme. The plaquette renormalization scheme reduces the amount of entanglement support between plaquettes by a factor of D compared with the exact contraction. This may bias toward those correlations compatible with the plaquette structure.

IV. CONCLUSION

We use the plaquette renormalization scheme to study spin-1/2 frustrated Heisenberg J_1-J_2 model on a square lattice with different sizes of $L = 8, 16$, and 32. Using the smallest possible bond dimension $D = 2$ for the underlying tensors, we are already able to obtain results beyond the mean-field theory. Since our method is variational, and the calculations are done on finite lattices, we are able to perform finite-size scaling to extrapolate the order parameters in the thermodynamic limit. We observe signatures of a continuous transition at $J_2^{c_1} \simeq 0.40J_1$, and a first-order phase transition at $J_2^{c_2} \simeq 0.62J_1$, consistent with previous numerical calculations.[14,21] Our calculations on the NN spin-spin correlation and the plaquette-order parameter indicates a possible plaquette VBS order for $J_2^{c_1} < J_2 < J_2^{c_2}$. The effects of the plaquette renormalization scheme and the bond dimension D dependence of the physical observables require further studies and will be presented in a future work.[44,45]

Note added. After submitting this manuscript, we recently learned of the DMRG work by Jiang *et al*.[46] and the tensor product state approach by Wang *et al*.[47] on the same model, which argue that the ground state in the nonmagnetic regime near $J_2/J_1 \sim 0.5$ could be a Z_2 spin liquid.

ACKNOWLEDGMENTS

We thank A. Sandvik for useful conversation and collaboration on related work. We are grateful to National Center for High-Performance Computing, and Computer and Information Networking Center, National Taiwan University (NTU) for the support of high-performance computing facilities. This work was partly supported by the National Science Council in Taiwan through Grants No. 100-2112-M-002-013-MY3 and No. 100-2120-M-002-00 (Y.J.K.), and by NTU Grants No. 99R0066-65,99R0066-68 and No. 10R80909-4 (J.F.Y., Y.J.K.). Travel support from National Center for Theoretical Sciences is also acknowledged.

*yjkao@phys.ntu.edu.tw

[1] P. W. Anderson, Mater. Res. Bull. **8**, 153 (1973).
[2] N. Read and S. Sachdev, Phys. Rev. Lett. **66**, 1773 (1991).
[3] F. Figueirido, A. Karlhede, S. Kivelson, S. Sondhi, M. Rocek, and D. S. Rokhsar, Phys. Rev. B **41**, 4619 (1990).
[4] L. Capriotti, F. Becca, A. Parola, and S. Sorella, Phys. Rev. Lett. **87**, 097201 (2001).
[5] P. Chandra and B. Doucot, Phys. Rev. B **38**, 9335 (1988).
[6] E. Dagotto and A. Moreo, Phys. Rev. Lett. **63**, 2148 (1989).
[7] H. J. Schulz and T. A. L. Ziman, Europhys. Lett. **18**, 355 (1992).
[8] M. E. Zhitomirsky and K. Ueda, Phys. Rev. B **54**, 9007 (1996).
[9] A. E. Trumper, L. O. Manuel, C. J. Gazza, and H. A. Ceccatto, Phys. Rev. Lett. **78**, 2216 (1997).
[10] R. F. Bishop, D. J. J. Farnell, and J. B. Parkinson, Phys. Rev. B **58**, 6394 (1998).
[11] L. Siurakshina, D. Ihle, and R. Hayn, Phys. Rev. B **64**, 104406 (2001).
[12] R. R. P. Singh, W. Zheng, J. Oitmaa, O. P. Sushkov, and C. J. Hamer, Phys. Rev. Lett. **91**, 017201 (2003).
[13] M. Mambrini, A. Lauchli, D. Poilblanc, and F. Mila, Phys. Rev. B **74**, 144422 (2006).
[14] J. Richter and J. Schulenburg, Eur. Phys. J. B **73**, 117 (2010).
[15] J. Reuther and P. Wölfle, Phys. Rev. B **81**, 144410 (2010).
[16] Y. Kamihara, T. Watanabe, M. Hirano, and H. Hosono, J. Am. Chem. Soc. **130**, 3296 (2008).
[17] T. Yildirim, Phys. Rev. Lett. **101**, 057010 (2008).
[18] Q. Si and E. Abrahams, Phys. Rev. Lett. **101**, 076401 (2008).
[19] F. Ma, Z.-Y. Lu, and T. Xiang, Phys. Rev. B **78**, 224517 (2008).
[20] M. P. Gelfand, R. R. P. Singh, and D. A. Huse, Phys. Rev. B **40**, 10801 (1989).
[21] V. N. Kotov, J. Oitmaa, O. P. Sushkov, and Z. Weihong, Phys. Rev. B **60**, 14613 (1999).
[22] R. R. P. Singh, Z. Weihong, C. J. Hamer, and J. Oitmaa, Phys. Rev. B **60**, 7278 (1999).
[23] O. P. Sushkov, J. Oitmaa, and Z. Weihong, Phys. Rev. B **63**, 104420 (2001).
[24] V. Murg, F. Verstraete, and J. I. Cirac, Phys. Rev. B **79**, 195119 (2009).
[25] L. Capriotti and S. Sorella, Phys. Rev. Lett. **84**, 3173 (2000).
[26] A. Läuchli, J. C. Domenge, C. Lhuillier, P. Sindzingre, and M. Troyer, Phys. Rev. Lett. **95**, 137206 (2005).
[27] E. Y. Loh, J. E. Gubernatis, R. T. Scalettar, S. R. White, D. J. Scalapino, and R. L. Sugar, Phys. Rev. B **41**, 9301 (1990).
[28] S. R. White, Phys. Rev. Lett. **69**, 2863 (1992).
[29] F. Verstraete and J. I. Cirac, e-print arXiv:cond-mat/0407066.
[30] T. Nishino, K. Okunishi, Y. Hieida, N. Maeshima, and Y. Akutsu, Nucl. Phys. B **575**, 504 (2000).
[31] G. Vidal, Phys. Rev. Lett. **99**, 220405 (2007).
[32] Z.-C. Gu, M. Levin, and X.-G. Wen, Phys. Rev. B **78**, 205116 (2008).
[33] H. C. Jiang, Z. Y. Weng, and T. Xiang, Phys. Rev. Lett. **101**, 090603 (2008).
[34] L. Wang, Y.-J. Kao, and A. W. Sandvik, Phys. Rev. E **83**, 056703 (2011).
[35] Z. Y. Xie, H. C. Jiang, Q. N. Chen, Z. Y. Weng, and T. Xiang, Phys. Rev. Lett. **103**, 160601 (2009).

[36]H. H. Zhao, Z. Y. Xie, Q. N. Chen, Z. C. Wei, J. W. Cai, and T. Xiang, Phys. Rev. B **81**, 174411 (2010).
[37]R. Brent, *Algorithms for Minimization without Derivatives* (Dover, Mineola, 2002).
[38]C. Liu, L. Wang, A. W. Sandvik, Y.-C. Su, and Y.-J. Kao, Phys. Rev. B **82**, 060410 (2010).
[39]A. W. Sandvik, Phys. Rev. B **56**, 11678 (1997).
[40]P. Hasenfratz and F. Niedermayer, Z. Phys. B **92**, 91 (1993).
[41]H. J. Schulz, T. A. L. Ziman, and D. Poilblanc, J. Phys. I **6**, 675 (1996).
[42]J. Sirker, Z. Weihong, O. P. Sushkov, and J. Oitmaa, Phys. Rev. B **73**, 184420 (2006).
[43]A. W. Sandvik and H. G. Evertz, Phys. Rev. B **82**, 024407 (2010).
[44]J. Yu, H.-C. Hsiao, and Y.-J. Kao, Computers & Fluids **45**, 55 (2011).
[45]J. Yu and Y.-J. Kao (unpublished).
[46]H.-C. Jiang, H. Yao, and L. Balents, e-print arXiv:1112.2241 (to be published).
[47]L. Wang, Z.-C. Gu, X.-G. Wen, and F. Verstraete, e-print arXiv:1112.3331 (to be published).